

M. GODEC

ISSN 0543-5846

METABK 52(3) 403-409 (2013)

UDC – UDK 621.385.833:535.33:535.42:543/545=111

PROGRESS IN THE USE OF THE MODERN RESEARCH EQUIPMENT AT THE INSTITUTE OF METALS AND TECHNOLOGY IN LJUBLJANA

Received – Prispjelo: 2012-09-23

Accepted – Prihvačeno: 2012-12-26

Review Paper – Pregledni rad

The installations of the modern research equipment at the Institute of Metals and Technology are presented chronologically, with an emphasis on electron microscopes with analytical techniques and spectroscopic methods. In parallel with the analytical techniques, there is a focus on the significance of the results for industry as well as their scientific impact.

Key words: electron microscopy, electron microanalysis, electron-backscatter diffraction

INTRODUCTION

Since its establishment in 1948, the Institute of Metals and Technology (IMT, formerly known as the Metallurgical Institute, MIL) has played a leading role in the field of materials characterization. As a result, it has always been among the first to implement the most advanced techniques and equipment into its research activities. Techniques that enable the characterization of materials are essential for engineers and scientists in research and development as well as in the control and testing of materials. There are many techniques, from the simple to the most sophisticated, and most of them were implemented at IMT for research very early, and IMT was often the first in the region to begin using some of these techniques.

Since the establishment of IMT in 1948, **optical metallography** has been one of the most important techniques used to characterize the structure of materials by revealing the grain boundaries, the phase boundaries, the distribution of inclusions and evidence of mechanical deformation. Image analysis (the quantitative analysis of geometrical properties) was implemented in microstructure analysis to minimize the influence of operator fatigue, which reduces the reproducibility and accuracy of manual measurements. Furthermore, with the era of digital cameras, progress in image analysis has made a significant step forward.

Electron probe microanalysis (EPMA) enables us to combine structural and compositional analyses in a single operation [1-3]. The first electron probe microanalysis (EPMA) was demonstrated at the University of Paris in 1948 [4]. In 1969, the first EPMA in Yugoslavia started working at IMT. Since then, IMT has played a leading role in **electron optical methods** in this region. In 1977 the first scanning electron microscope (SEM) was in-

stalled at IMT. This was very early; especially if we consider that the first commercial SEM became available in 1965. The first field-emission scanning electron microscope in Slovenia was installed at IMT in 2004. A FEG SEM as a source of electrons for Auger electron spectroscopy was in operation even earlier, from 1997.

The first Auger electron spectrometer (AES) started to work at the IEVT institute in Ljubljana 1977, while at IMT an improved AES with XPS analysis was installed 1997. Both techniques are **electron and X-ray spectroscopic methods** [5], respectively, and are surface sensitive and therefore crucial for surface and grain-boundary studies [6]. The AES and XPS techniques also enable the study of fracture surfaces due to the possibilities to fracture bulk specimens in an ultra-high vacuum [7].

The first electron-diffraction-based technique in SEM was again first put into operation at IMT. In 2005, the electron-backscatter diffraction technique (EBSD) was added to the FE SEM, which had been acquired one year earlier. The electron-backscatter pattern is formed due to the interactions of incident electrons with the crystal structure of the analyzed matter. The phenomenon has been known since 1954; however, some modifications were made to improve the quality of the patterns [8,9]. The EBSD technique is used for orientation determinations, phase identifications and strain measurements [10-13].

In 1999, IMT started using commercial software for image analysis, which became a standard tool for quantitative microstructure analysis.

PROGRESS IN THE USE OF MODERN RESEARCH EQUIPMENT AT IMT EPMA

In the region of the former Yugoslavia, a line-scan of the segregation in steel was first presented [14] in 1958

M. Godec, Institute of Metals and Technology, Ljubljana, Slovenia

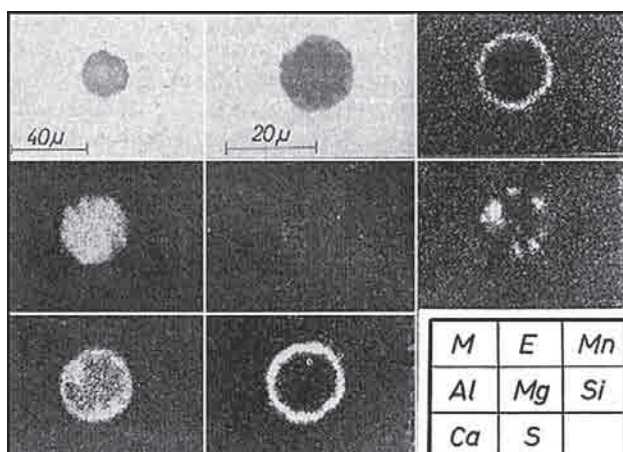


Figure 1 Spherical, non-metallic inclusion in construction steel (mapping) rich in aluminium, silicon and calcium in the middle, surrounded by a membrane of calcium-sulphide [17]

at the first International Colloquium on Residuals in Iron and Steel, organized jointly by institutes from France, Germany and Yugoslavia. Scientists from Yugoslavia started to use EPMA line scanning in 1962 and image scanning in 1967 [15,16]. The first EPMA started working in 1969 at MIL (Metallurgical Institute Ljubljana) and the first result was a map analysis of non-metallic inclusions of manganese sulphide and aluminium oxide. Results that were significant for the development of industrial technology and science (Figure 1) were achieved relatively soon [17]. It was found that the calcium in a construction steel melt reacts with other non-metallic inclusions and does not evaporate from the steel melt. This was one of the first X-ray maps obtained using EPMA in Europe.

Based on EPMA some very significant results were obtained (Figure 2) concerning the homogenisation of chromium in steel with 1 % C and 1,5 % Cr [18]. It was found that the chromium segregation cannot be totally homogenised, because the reaction is driven by the activity of chromium and carbon in an austenite solid solution.

In 1975 a survey of previous work was published [19]. A few years later a level of sensitivity equal to 10 ppm was achieved by quantitative analyses. Already in 1969, the use of EPMA analysis had spread to industry and research institutions in the whole of Yugoslavia and the results started to be used in research aimed at improving steel, aluminium, and copper alloys, as well as in basic research in solid-phase chemistry, the physics of solids, geology and even dentistry. Based on the EPMA results the evolution of the composition of non-metallic inclusions in steel was explained and better controlled, the homogenization time for several aluminium and copper alloys was shortened by half, and the binary equilibrium diagrams for the carbides TiC and NbC and transition metals as well as some ceramic compounds were determined. It was also discovered that for a proper analysis of some types of glass, a larger electron beam diameter must be used to obtain a reliable

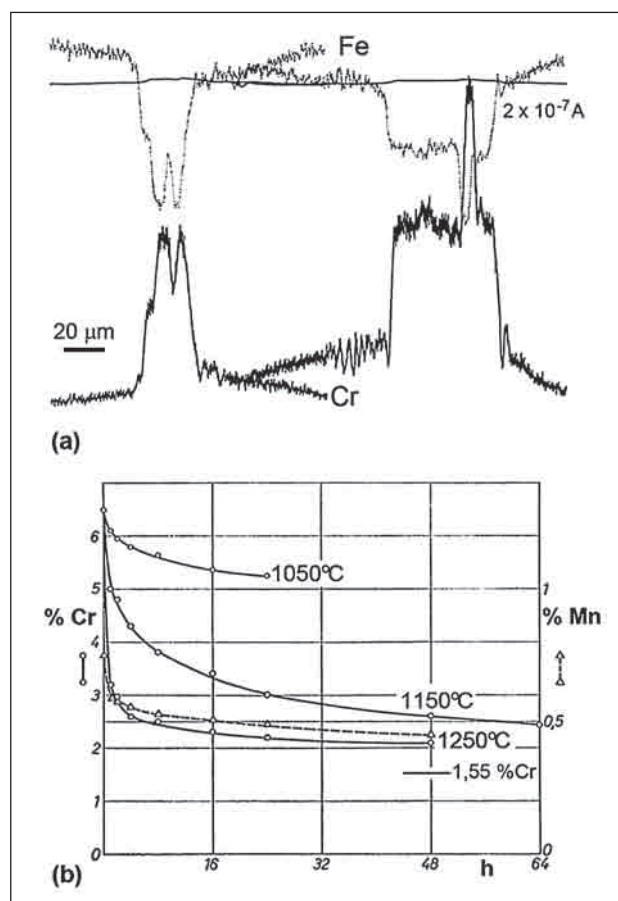


Figure 2 (a) EPMA line scan of chromium and iron in a eutectic phase in steel with 1 % C and 1,5 % Cr. The composition corresponds to two carbides: Fe_3C with chromium, which grows into the inner eutectic field up to 21 % chromium; and a small carbide M_{23}C_6 which contains 55 mas % iron. (b) Homogenization diagram [18]

quantitative composition. After a few years EPMA was also acquired by research institutions and universities in Zenica, Sisak and Belgrade as well as at the Jožef Stefan Institute in Ljubljana.

The use of TEM and replica methods became insufficient for projects related to micrometer-sized and smaller microstructure features in alloys and fracturing micromorphology, and so in 1978 a SEM equipped EPMA and image analysis was acquired at MIL. Also, the use of similar SEMs expanded rapidly and several SEM+EPMA devices were in operation in Yugoslavia. A very significant achievement based on the explanation of fracturing events, properties and the change of properties with operating time in parts of thermal power stations was obtained.

AES/XPS Techniques

Answers to questions related to the change of properties and microstructure related to grain-boundary and surface segregations could not be provided by analyses with the available analytical devices as the depth of generation of the signal on the EPMA was much greater than the thickness of the segregation and an Auger elec-

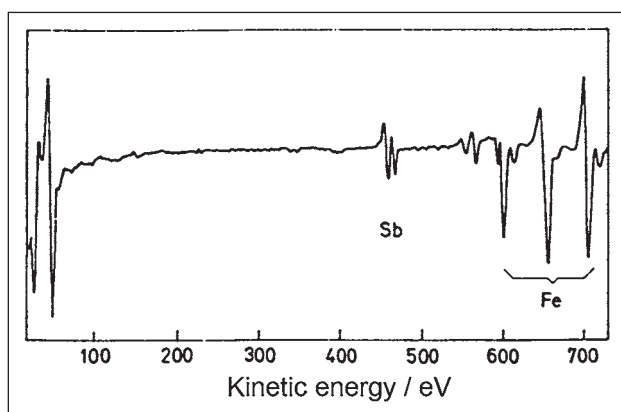


Figure 3 AES differential spectra of maximum equilibrium antimony segregation obtained at 700 °C on the surface of non-oriented electrical steel alloyed with 0.05 % Sb [20].

tron spectrometer (AES) became necessary. Therefore, a combined SEM/AES/XPS instrument, which enables SEM imaging of the sample surface, local AES analysis within the imaged area as well as XPS analysis of wider areas, was acquired and put into operation. New analytical results and images were used in basic and applied research projects, for instance the effect of the alloy composition, temperature and time on antimony, copper and tin surface segregation on the recrystallisation of grains and the texture of soft magnetic sheets; the effect of tempering temperature on phosphorus segregation; and the properties of heat-treated steel. It was shown that the segregation of certain elements from the IV A to the VI A group enriches the surface and the grain boundary. Thus, by segregation, the surface energy decreases selectively, and so the difference in the total energy of the grain, which is the driving force for its growth during recrystallisation, causes selective grain growth with a different spatial orientation. Figure 3 shows antimony enrichment caused by equilibrium segregation on the surface of non-oriented electrical steel [20]. Using AES techniques for segregation kinetics studies and the X-ray diffraction method for texture analysis, it was shown that a certain amount of tin has a positive effect on the texture development [21].

The electron spectroscopy technique AES was successfully applied in the characterization of plasma-assisted chemical vapour deposition (PACVD) TiN/Ti(B-N)/TiB₂ coatings for hot-worked tool steels. Such surface treatments are used for die casting and forging tools where high wear performances have to be achieved with multi hard films. The understanding of their composition is important to develop such multi nano-layers. AES depth profiling through such a multi-films layer is shown in Figure 4 [22].

The AES technique is surface sensitive, which also enables a very small lateral resolution of detection. XPS is surface sensitive as well, but with a lower lateral resolution. However, it gives information about the chemical state of the analysing elements due to chemical shifts in the spectra. Using XPS analyses it was possible to

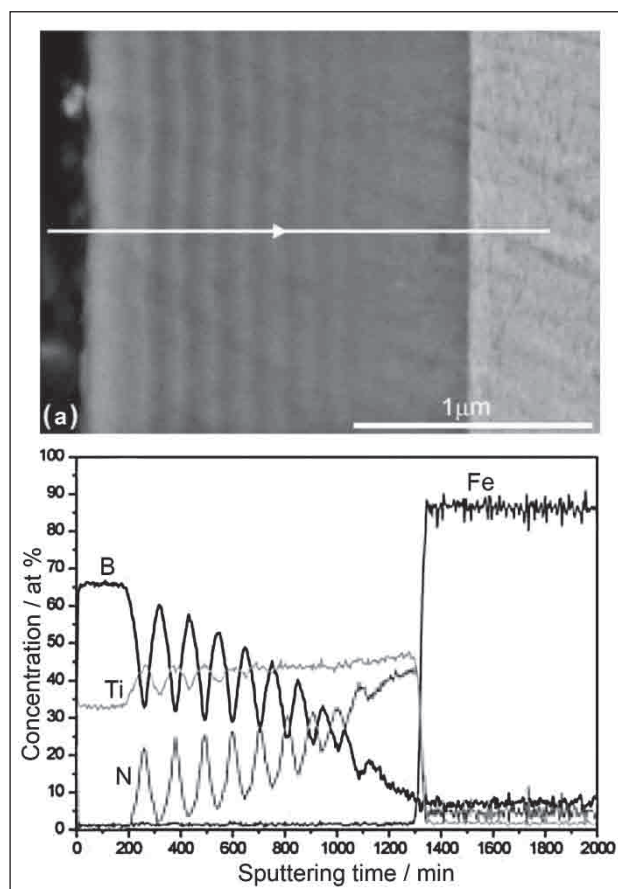


Figure 4 AES sputter depth profile of the TiN/Ti(B-N)/TiB₂ multi-layered hardcoatings; (a) BE image showing the region of the AES depth profile, (b) AES sputter depth profile of the profile of the TiN/Ti(B-N)/TiB₂ coatings showing an approximate 15 nm depth resolution [22]

obtain information about the chemical states of hip prosthesis on rough and polished regions after the prosthesis had been removed from a patient as a result of aseptic loosening. The XPS results show small differences between the rough and polished surfaces. The passive layers established on the surface of both regions contained the oxides of two main elements, i.e., Fe and Cr. The oxides of the alloying elements Ni and Mo, also contributed to the passive layer. Calcium phosphate was also detected on both surfaces. Figure 5 shows a detailed XPS scan over these selected binding-energy ranges for the polished surface of the hip prostheses.

AES and XPS were also applied to study ultra-thin oxide layers and their formation on polished and sputter-cleaned duplex stainless-steel samples. In one such study [24] these samples were exposed to 10⁻⁵ mbar of pure oxygen inside the vacuum chamber, or exposed to ambient conditions for 24 h, or plasma oxidized. The oxide layers thus produced were analyzed by XPS depth profiling to determine the oxide layers' chemical and chemical-state compositions with depth (Figure 6 and 7). It was found that all the formation methods produced oxide layers with thicknesses in the range of nanometers with different traces of metallic components and with the maximum concentration of chromium oxide shifted

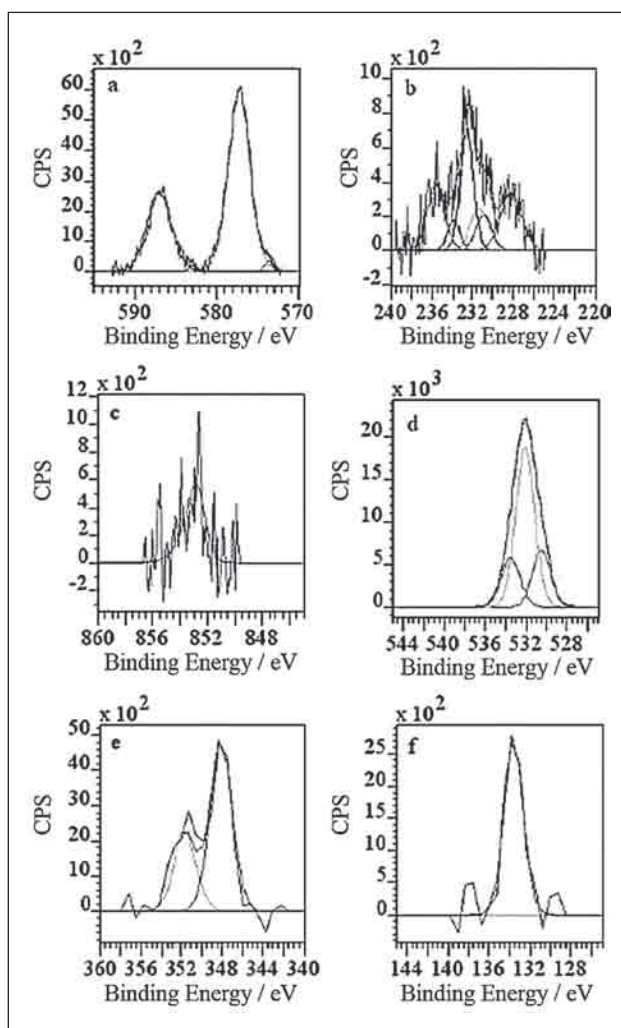


Figure 5 High-resolution XPS spectra from the polished-type surface; Cr 2p (a), Mo 3d (b), Ni 2p (c), O 1s (d), Ca 2p (e), P 2p (f) [23]

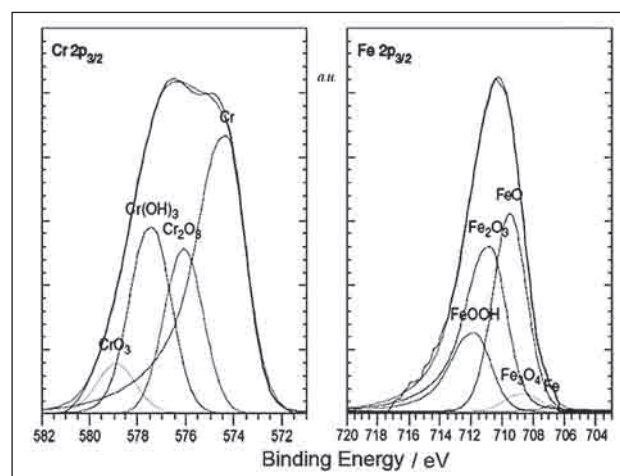


Figure 6 Cr 2p_{3/2} and Fe 2p_{3/2} high-resolution XPS spectra fitted with components corresponding to the different chemical states of Cr and Fe [24]

towards the oxide-layer-bulk-metal interface. A common characteristic of all the oxide layers investigated was a double-oxide stratification, with regions closer to the surface exhibiting higher concentrations of iron oxide and those more in-depth exhibiting higher concentrations of chromium oxide (Figure 7 and 8). AES and XPS were also used in the analysis of Ni-Ti based medical shape memory alloys [25].

SEM/EBSD Technique

Reliable answers related to the effect of microstructure and the heat treatment of metals were sometimes questionable because of the problems related to the lack of a methodology for a reliable assessment of the space

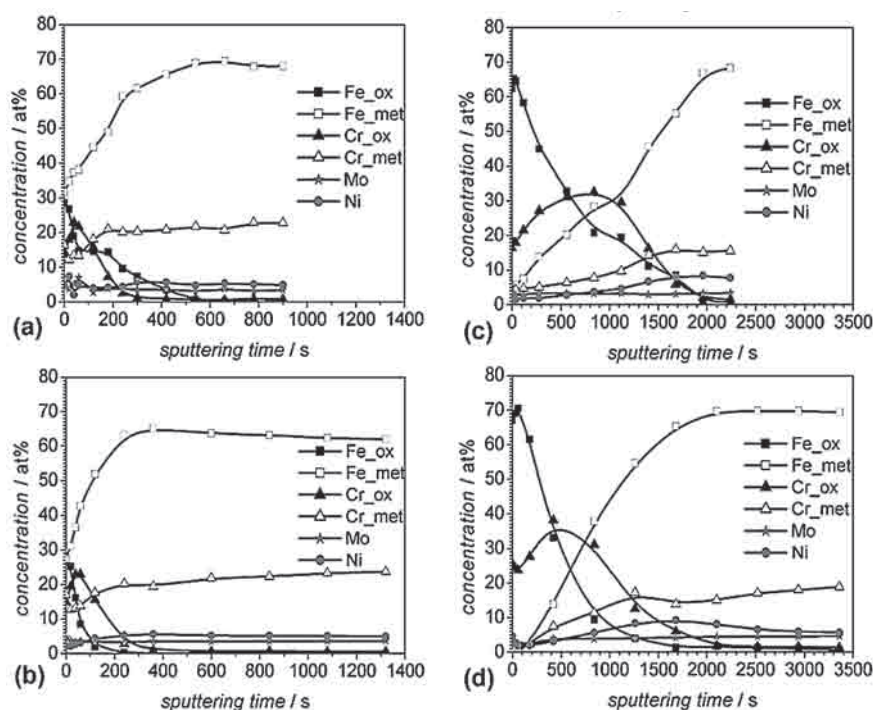


Figure 7 XPS depth profile at 90 L exposure in the preparation chamber (a), at 10800 L exposure in the preparation chamber (b), of the sample oxidized in ambient conditions for 24 hours (c) and of the sample oxidized in plasma (d) [24]

orientation of single grains. For this reason the newly acquired SEM+EPMA was equipped with an EBSD device, enabling a determination of the lattice space orientation of single grains in the microstructure of metals, the related lattice parameters and the possibility to deduce the elastic stresses related to the lattice parameters.

Significant new information on the relations between the lattice orientations of the constituents of the microstructure was obtained, for example, information about the carbide types forming in steels used for steam turbines, pipes and other components in power plants as well as their orientation relation to the matrix and a further change of the chemical and phase compositions. The EBSD analytical technique was also successfully applied to explain the transformation of carbides during the annealing of non-equilibrium solidifying high-speed steel. Using EBSD it was shown that in ledeburitic tool steel at too high a casting temperature and at too low a cooling rate the additional precipitation of carbides occurs, which significantly influences the workability of such steel [26]. Plenty of different EBSD texture analyses were performed in electrical steels in order to explain the influence of the alloying elements on the recrystallization. Last but not least, EBSD was used to detect the first-forming nano-crystal phase in amorphous soft magnetic powders and give an explanation of the orientations of the dendrite arms [27].

The EBSD technique was originally invented to analyse the texture of polycrystalline materials. At IMT we started using this technique to follow texture development in electrical steels that were produced at Acroni, Jesenice or to perform texture measurements on electrical steel grades manufactured at IMT.

We showed [28] that the higher core losses can be explained by texture development and that besides the

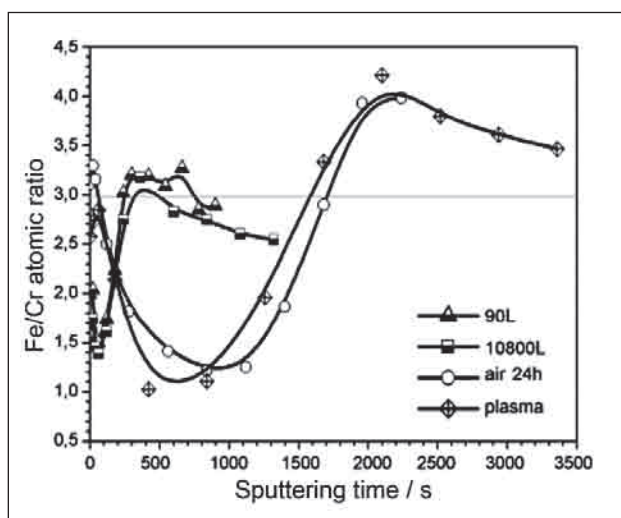


Figure 8 Fe/Cr atomic ratios calculated from XPS depth profiles for oxide layers prepared by 90 L exposure in the preparation chamber, 10800 L exposure in the preparation chamber, oxidation in ambient conditions for 24 hours and plasma oxidation (d). The horizontal line at 2,98 represents the calculated Fe/Cr atomic ratio in bulk DSS 2205 [24]

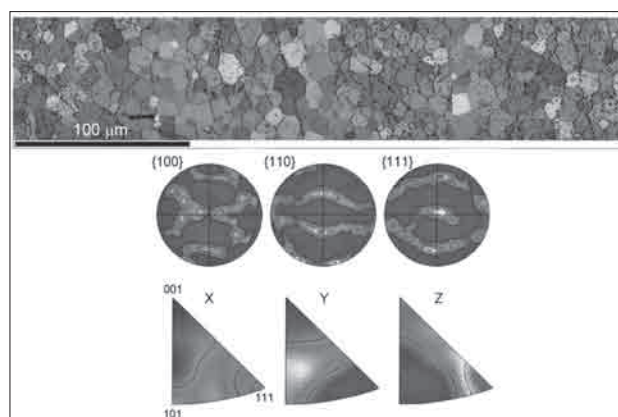


Figure 9 EBSD orientation maps of microstructures as well as the {100}, {110} in {111} pole figures and the {100}, {110}, {111} inverse pole figures of the sample with a lower core loss [28]

microstructural components, the nanostructure and nanoprecipitates also have a crucial impact on the magnetic properties. In Figure 9 some texture results presented in key colour mode, pole figures and inverse pole figures are shown.

A lot of very important results for industrial applications were achieved by using EBSD techniques as a phase-analysis technique. Ledeburitic tool steels have a relatively low workability. Selecting the correct casting and soaking temperatures as well as the cooling rate during solidification improves the intrinsic hot workability of some tool steels because these parameters influence the crystallization, precipitation, dissolution, growth, distribution, fraction, size, and type of carbides [26]. Figure 10 shows the evolution of the microstructure at a certain cooling rate.

IMT has a long tradition in researching the fields of steels and other materials used in power plants as pipe-work, boilers and different turbine blades. Using the FE SEM equipped with EBSD and TEM the microstructures of creep-resistant steels exposed to high temperatures for long periods were studied and some explanations were proposed in order to predict the lifetime of different critical elements in the power-generating industry. The FE SEM enabled us to reveal all the details in the microstructures, for instance carbide precipitates as well as carbonitrides and some other phases (Figure 11). Based on the EBSD analysis it was shown that nano-carbide particles could be detected and determined (Figure 12) and also the related space orientation of the carbides to the matrix phase (Figure 13) [29].

Our researchers proposed an improved power-law, stress-dependent, energy-barrier model for 9Cr–1Mo–0.2V steel using short-term creep data (the small-punch method) [30]. Based on all these results we are developing a theoretical and semi-empirical dependency of the carbide precipitates' growth rate on the composition and the temperature, and we are developing an improved and reliable relationship between size, spacing and carbide volume ratio, and creep rate.

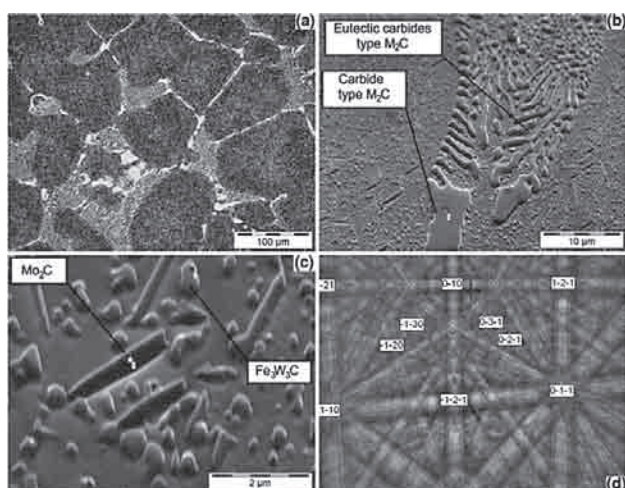


Figure 10 Microstructure obtained at a cooling rate of 0,25 K/s for the AISI M42 tool steel. The spots show the locations of the EBSD analyses: the coarser lamellar eutectic type M_2C , the blocky carbides type M_2C and the spheroidized carbides type M_6C in ferrite and the sticks of type Mo_2C ; (a) OM, (b) SEM, (c) EBSD, and (d) Kikuchi pattern for Fe_3W_3C , spot 1 in (c) [26]

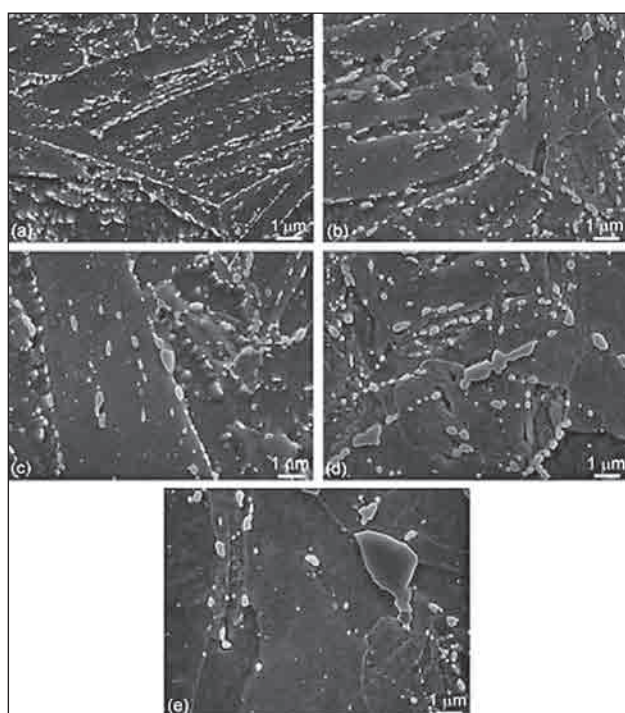


Figure 11 SE images of the microstructure of X20CrMoV12.1 steel (a) in the initial state and after annealing at 800 °C for (b) 3 h, (c) 7 h, (d) 24 h and (e) 168 h [29]

A model based on micromechanical modelling and the modelling of microstructure evolution during operation is also being developed and this will have a great impact in the field of creep-resistance prediction and the assessment of the remaining lifetime for critical components operating in thermal power plants.

Using EBSD we proposed a method to assess the volume fraction of different carbides in steels. This can be done by capturing the image in the SEM in backscatter mode (BEI) using a high current of the electron beam

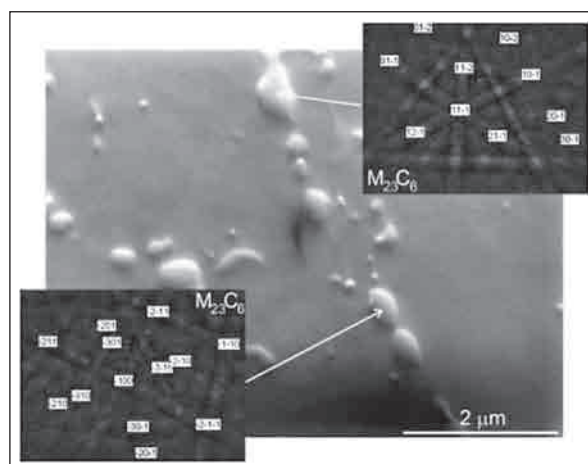


Figure 12 SE image of the specimen annealed for 24 h at 800 °C and the corresponding EBSD patterns of two carbides solved as $M_{23}C_6$ [29]

(Figure 14) and separating different phases by defining the correct thresholds in the grey-scale histogram in the SE or BE image using image-analysis software. On the other hand, it can be done by EBSD mapping or even using a band-slope map, which shows the Kikuchi pattern quality, and use the fact that the martensitic phase has a poor Kikuchi pattern [31]. Figure 15 shows some steps in the image analysis to obtain the separation of three different phases and to obtain the volume fraction of each phase.

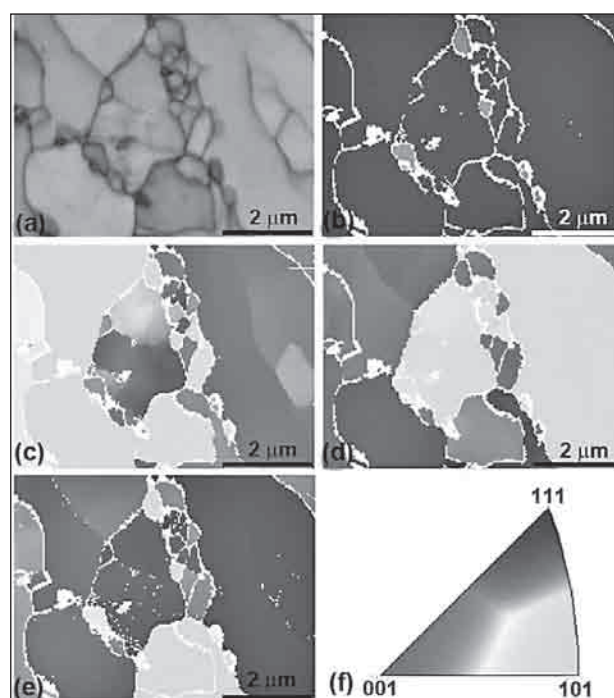


Figure 13 EBSD orientation mapping of the specimen annealed for 24 hours at 800 °C: (a) band-contrast image; (b) phasemap (blue - ferrite phase, red - $Cr_{23}C_6$ phase); (c) IPFs colouring in the x direction; (d) IPFs colouring in the y direction; (e) IPFs colouring in the z direction and (f) colour legend for the cubic system [29].

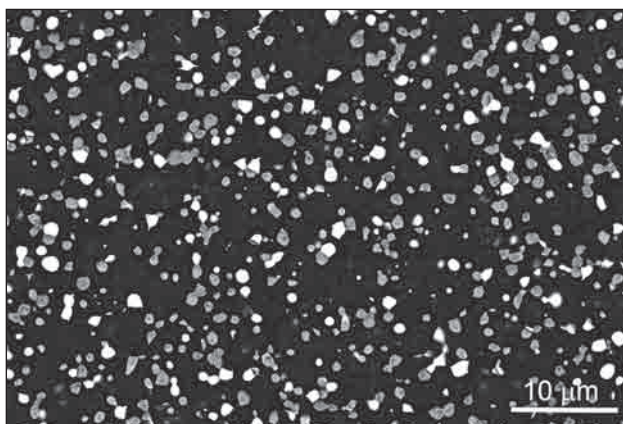


Figure 14 BE image of polished S390 Microclean steel surface [31]

CONCLUSION

The Institute of Metals and Technology (IMT), formerly known as the Metallurgical Institute (MIL), has, throughout its history, invested heavily in state-of-the-art research equipment and, what is even more important, invested in the knowledge to use such sophisticated equipment. Therefore, IMT was, and still is, one of the leading institutes in the field of metallic materials in the region. The researchers at IMT that have been using electron optical methods (EPMA, FE SEM equipped with EDS, WDS and EBSD) and electron and X-ray spectroscopic methods (AES and XPS) have been providing industry with excellent support and also providing an innovative approach and an increase in theoretical and applied knowledge in the field of metallurgy and material science as well as in interdisciplinary fields and published them in numerous research articles.

Acknowledgements

The author would like to express his gratitude to prof. dr. F. Vodopivec and prof. dr. M. Jenko for their permission for the use of the images and diagrams previously published.

REFERENCES

- [1] K. F. J. Heinrich, *Adv. Opt. Elec. Microsc.*, 6 (1981) 275-301.
- [2] R. Fitzgerald, K. Keil, K.F.J. Heinrich, *Science* 159 (1968) 528-534.
- [3] J. I. Goldstein, D. E. Newbury, p. Echlin, D. C. Joy, C. Fiori, E. Lifshin, *Scanning Electron Microscopy and X-ray Microanalysis*, Plenum Press, 1985, p1.
- [4] R. Castaing, Thesis, University of Paris, France, 1951.
- [5] D. Briggs, M.P. Seah (Eds.), *Practical Surface Analysis: Auger and X-ray Photoelectron Spectroscopy*, second ed., vol. 1, Wiley, Chichester, 1990, p1.
- [6] T. Muschik, S. Hofmann, W. Gust, *Scripta Metallurgica*, 22 (1988) 3, 349-354.
- [7] H. Viehhaus, R. Möller, H. Erhart, H. J. Grabke, *Scripta Metallurgica*, 17 (1983) 2, 165-170.
- [8] D. J. Dingley, *Scanning Electron Microscopy*, 2 (1984), 569-575.
- [9] D. J. Dingley, *Institute of Physics Conference Series*, 98 (1989), 473-476.

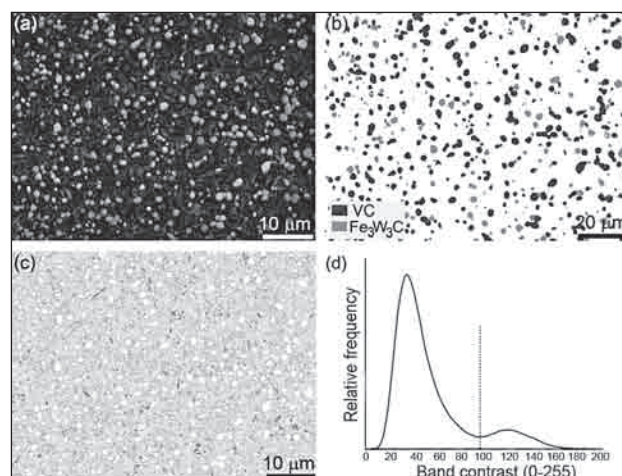


Figure 15 EBSD maps. (a) Band-contrast image, (b) phase image, (c) rainbow colour image, (d) band-contrast histogram [31]

- [10] A. J. Schwartz, M. Kumar, B. L. Adam (Eds), *Electron-backscatter diffraction in materials science*, New York: Kluwer Academic, 2000.
- [11] C. L. Chen, R.C. Thomson, *Journal of Alloys and Compounds*, 490 (2010), 293-300.
- [12] M. Kamaya, *Materials Characterization*, 66 (2012) 56-67.
- [13] J.C. Huang, I.C. Hsiao, T.D. Wang and B.Y. Lou, *Scripta Materialia*, 43 (2000), 213-220.
- [14] C. Crussard, A. Kohn, C. de Beulieu, J. Philibert, *Zbornik Colloque de Portorož*, (1958), 395-406
- [15] F. Vodopivec, A. Kohn, J. Philibert, J. Manenc, *Memoires Scientifiques de la Revue de Métallurgie*, 60 (1963), 11, 802-818.
- [16] L. Kosec, F. Vodopivec, R. Tixier, *Métaux-Corrosion-Industries*, 525 (1969), 1-25.
- [17] F. Vodopivec, B. Ralič, *Železarski Zbornik*, 6 (1972), 215-229.
- [18] F. Vodopivec, B. Ralič, *Železarski Zbornik*, 8 (1974), 217-222.
- [19] F. Vodopivec, B. Ralič, *Einige praktische Erfahrungen mit der quantitativen Elektronen-Strahl-Mikroanalyse von Stählen*, *Radex Rundschau*, (1975), 289-294
- [20] M. Jenko, F. Vodopivec, M. Godec, D. Steiner Petrovič, *J. phys.*, IV (Les Ulis), 5 (1995), C7 225-231.
- [21] M. Godec, M. Jenko, *ISI int.*, 39 (1999), 7, 742-746.
- [22] M. Jenko, Dj. Mandrino, M. Godec, J.T. Grant, V. Leskovšek, *Mater. tehnol.*, 42 (2008) 6, 251-255.
- [23] M. Godec, A. Kocijan, D. Dolinar, Dj. Mandrino, M. Jenko, V. Antolič, *Biomedical materials*, 5 (2010) 5, 4-11.
- [24] C. Donik, A. Kocijan, Dj. Mandrino, I. Paulin, M. Jenko, B. Pihlar, *Appl. Surf. Sc.*, 255 (2009) 15, 7056-7061.
- [25] M. Jenko, J. T. Grant, R. Rudolf, T. Kokalj, Dj. Mandrino, *Surface and Interface Analysis*, 44 (2012), 8, 997-1000.
- [26] T. Večko Pirtovšek, G. Kugler, M. Godec, M. Terčelj, *Metall. mater. trans., A Phys. metall. mater. sci.*, 43A (2012), 3797-3808.
- [27] M. Godec, D. Nolan, M. Jenko, *Mater. sci. eng., B, Solid-state mater. adv. technol.* 129B (2006) 1, 31-38.
- [28] D. Steiner Petrovič, M. Godec, B. Markoli, M. Čeh, *J. magn. magn. Mater.*, 322 (2010) 20, 3041-3048.
- [29] D. A. Skobir Balantič, M. Godec, A. Nagode, M. Jenko, *Surf. interface anal.*, 42 (2010) 6/7, 717-721.
- [30] B. Ule and A. Nagode, *Scripta Materialia*, 57 (2007) 405-408.
- [31] M. Godec, B. Šetina, Dj. Mandrino, A. Nagode, V. Leskovšek, D. Škapin, M. Jenko, *Mater. charact.* 61 (2010) 4, 452-458,

Note: The responsible translator for English language is P. McGuines, IJS, Ljubljana, Slovenia